

Synthesis, structure and magnetic properties of an amine-templated Mn^{2+} ($S = 5/2$) sulfate with the Kagome structure

J. N. Behera^{a,b} and C. N. R. Rao^{*a,b}

Received 21st September 2006, Accepted 4th January 2007

First published as an Advance Article on the web 15th January 2007

DOI: 10.1039/b613732f

In pursuit of a compound with the Kagome structure, formed by a non- Fe^{3+} transitional metal ion with a spin of $5/2$, we have synthesized an amine-templated Mn^{2+} sulfate under solvothermal conditions. This compound with a perfect Kagome structure shows evidence for antiferromagnetic interactions with no long-range order.

Introduction

Transition metal compounds with the Kagome structure are not only interesting structurally but also because of their magnetic properties. There have been several studies of Kagome compounds of Fe^{3+} ($S = 5/2$) such as the jarosites, in the past few years, all of which exhibit magnetic frustration or low-temperature antiferromagnetism.¹ The Fe^{3+} jarosites are generally not pure owing to the presence of site defects. Nocera *et al.*² have recently prepared a pure Fe^{3+} jarosite by redox-based hydrothermal methods and found the Fe^{3+} Kagome layer in this compound shows an antiferromagnetic transition at 61.4 K. On the other hand, V^{3+} ($S = 1$) and Ni^{2+} ($S = 1$) Kagome compounds appear to show the presence of ferromagnetic interaction and less evidence of frustration.^{3,4} A theoretical study employing quantum many-body Heisenberg models has shown that Kagome compounds where transition metal ions with half-odd integer spins would exhibit magnetic-frustration while those with transition metal ions with integral spins may show evidence for ferromagnetic interactions and less of frustration.⁵ In view of the above observation, we considered it as important to prepare a Kagome compound with a transition metal ion other than Fe^{3+} , with $S = 5/2$. We have now been able to synthesize an amine-templated manganese(II) sulfate of the composition, $[\text{C}_4\text{N}_2\text{H}_{12}][\text{NH}_4]_2[\text{Mn}^{\text{II}}_3\text{F}_6(\text{SO}_4)_2]$, **I**, with the Kagome structure, under solvothermal conditions. We describe the structure and magnetic properties of this compound in this article. Interestingly, we find that the magnetic properties of this compound differ from those of Fe^{3+} jarosites² as well as Kagome compounds where the transition metal ions have integral spins.^{3,4}

Results and discussion

The asymmetric unit (Fig. 1a) of **I** consists of 27 non-hydrogen atoms, out of which 19 belong to the inorganic-framework and 8 to the extra-framework guest molecules, including two nitrogens of the two ammonium ions. It consists of vertex-sharing $\text{Mn}^{\text{II}}\text{F}_4\text{O}_2$ octahedra and SO_4 tetrahedral units, which are fused together by Mn–F–Mn and Mn–O–S bonds. The distorted octahedron around

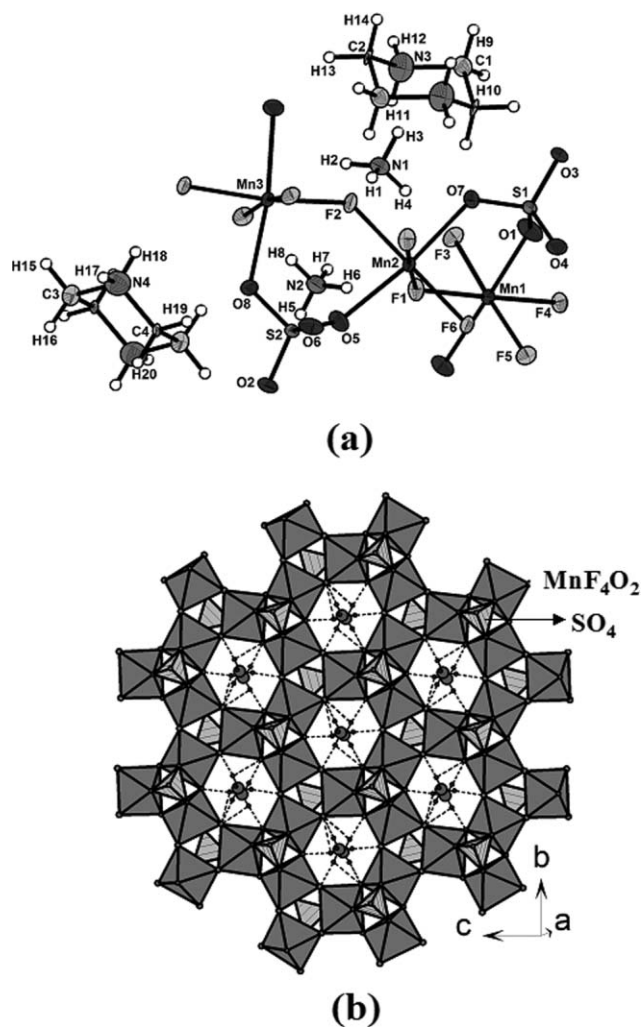


Fig. 1 (a) Labeled asymmetric unit of $[\text{C}_4\text{N}_2\text{H}_{12}][\text{NH}_4]_2[\text{Mn}^{\text{II}}_3\text{F}_6(\text{SO}_4)_2]$, **I**. Thermal ellipsoids are given at 50% probability. (b) Polyhedral view of the hexagonal Kagome layer in **I**. Note the presence of the ammonium ion in the hexagonal channel.

Mn^{2+} has the oxygen atoms from the sulfate along the z -axis and of the F atoms along the xy -plane. Each MnF_4O_2 unit shares four of its Mn–F vertices with similar neighbors, with the Mn–F–Mn bonds roughly aligned in the bc -plane. The Mn–O bond is

^aChemistry and Physics of Materials Unit, Jawaharlal Nehru Centre for Advanced Scientific Research, Jakkur P. O., Bangalore, 560064, India

^bSolid State and Structural Chemistry Unit, Indian Institute of Science, Bangalore, 560012, India. E-mail: cnrrao@jncasr.ac.in; Fax: +91-80-2208-2760

canted from the *bc*-plane and the Mn–O vertex forces a three-ring trio of apical Mn–O bonds close together to be capped by the SO₄ tetrahedra. The sulfate groups are positioned alternatively up and down about the hexagonal layer. The three- and six-rings of the octahedra forming the in-plane connectivity can be seen in Fig. 1(b). Such a layer consisting of a hexagonal tungsten bronze layer is characteristic of the Kagome structure.⁶

The Mn–O bond distances in **I** are in the range 2.179(3)–2.246(3) Å, [(Mn(1)–O)_{av} = 2.210(3), (Mn(2)–O)_{av} = 2.194(3) and (Mn(3)–O)_{av} = 2.236(3) Å]. The Mn–F bond distances are in

the range 2.097(2)–2.126(2) Å [(Mn(1)–F)_{av} = 2.110(2), (Mn(2)–F)_{av} = 2.116(2) and (Mn(3)–F)_{av} = 2.108(2) Å]. Selected values of the bond distances and bond angles in **I** are listed in Table 1. The values of the bond angles and distances indicate a distorted octahedral coordination of Mn and near-perfect tetrahedral coordination of sulfur. Bond valence sum calculations⁷ using *r*₀ (Mn–F) of 1.698 and *r*₀ (Mn–O) of 1.790 Å [Mn(1) = 1.95, Mn(2) = 1.96 and Mn(3) = 1.92] and the values of the bond distances indicate the valence state of the Mn atoms to be +2. The bond valence sums are also consistent with the presence of bridging fluorine

Table 1 Bond lengths [Å] and angles [°] for **I**^a

Mn(1)–F(1)	2.106(2)	Mn(3)–F(6)	2.108(2)
Mn(1)–F(2)	2.111(2)	Mn(3)–F(2)#2	2.108(2)
Mn(1)–F(3)	2.111(2)	Mn(3)–F(5)#3	2.122(2)
Mn(1)–F(4)	2.115(2)	Mn(3)–O(5)#3	2.227(3)
Mn(1)–O(1)	2.182(3)	Mn(3)–O(6)	2.246(2)
Mn(1)–O(2)#1	2.238(3)	S(1)–O(7)	1.461(3)
Mn(2)–F(3)#2	2.103(2)	S(1)–O(3)	1.464(3)
Mn(2)–F(1)	2.115(2)	S(1)–O(6)	1.480(3)
Mn(2)–F(5)	2.120(2)	S(1)–O(2)	1.485(3)
Mn(2)–F(6)	2.126(2)	S(2)–O(1)	1.458(3)
Mn(2)–O(3)	2.179(3)	S(2)–O(8)	1.467(3)
Mn(2)–O(4)	2.210(3)	S(2)–O(5)	1.477(3)
Mn(3)–F(4)#3	2.097(2)	S(2)–O(4)	1.478(3)
C(1)–C(2)#5	1.487(5)	C(3)–N(4)	1.513(5)
C(1)–N(3)	1.509(6)	N(4)–C(4)	1.479(5)
N(3)–C(2)	1.493(5)	C(4)–C(3)#6	1.485(5)
F(1)–Mn(1)–F(2)	178.76(9)	F(6)–Mn(3)–F(5)#3	172.67(8)
F(1)–Mn(1)–F(3)	87.89(9)	F(2)#2–Mn(3)–F(5)#3	88.14(8)
F(2)–Mn(1)–F(3)	90.93(8)	F(4)#3–Mn(3)–O(5)#3	104.36(9)
F(1)–Mn(1)–F(4)	94.06(8)	F(6)–Mn(3)–O(5)#3	89.45(10)
F(2)–Mn(1)–F(4)	87.12(8)	F(5)#3–Mn(3)–O(5)#3	83.73(9)
F(3)–Mn(1)–F(4)	177.59(9)	F(4)#3–Mn(3)–O(6)	89.08(9)
F(1)–Mn(1)–O(1)	92.49(10)	F(6)–Mn(3)–O(6)	103.02(9)
F(2)–Mn(1)–O(1)	87.12(9)	F(2)#2–Mn(3)–O(6)	82.08(9)
F(3)–Mn(1)–O(1)	88.34(10)	F(5)#3–Mn(3)–O(6)	84.23(9)
F(4)–Mn(1)–O(1)	90.17(10)	O(5)#3–Mn(3)–O(6)	162.17(11)
F(1)–Mn(1)–O(2)#1	85.41(9)	O(7)–S(1)–O(3)	110.76(16)
F(2)–Mn(1)–O(2)#1	94.99(9)	O(7)–S(1)–O(6)	109.61(15)
F(3)–Mn(1)–O(2)#1	92.26(9)	O(3)–S(1)–O(6)	108.77(16)
F(4)–Mn(1)–O(2)#1	89.30(9)	O(7)–S(1)–O(2)	109.51(15)
O(1)–Mn(1)–O(2)#1	177.79(10)	O(3)–S(1)–O(2)	109.57(16)
F(3)#2–Mn(2)–F(1)	176.59(8)	O(6)–S(1)–O(2)	108.59(16)
F(3)#2–Mn(2)–F(5)	85.59(8)	O(1)–S(2)–O(8)	111.17(16)
F(1)–Mn(2)–F(5)	91.80(9)	O(1)–S(2)–O(5)	109.51(17)
F(3)#2–Mn(2)–F(6)	91.99(9)	O(8)–S(2)–O(5)	108.58(15)
F(1)–Mn(2)–F(6)	90.62(9)	O(1)–S(2)–O(4)	109.57(17)
F(5)–Mn(2)–F(6)	177.57(8)	O(8)–S(2)–O(4)	109.28(15)
F(3)#2–Mn(2)–O(3)	99.11(9)	O(5)–S(2)–O(4)	108.69(16)
F(1)–Mn(2)–O(3)	83.27(9)	Mn(1)–F(1)–Mn(2)	129.15(10)
F(5)–Mn(2)–O(3)	94.36(10)	Mn(3)#1–F(2)–Mn(1)	130.99(10)
F(6)–Mn(2)–O(3)	85.88(10)	Mn(2)#1–F(3)–Mn(1)	126.04(10)
F(3)#2–Mn(2)–O(4)	88.32(10)	Mn(3)#4–F(4)–Mn(1)	123.99(10)
F(1)–Mn(2)–O(4)	89.73(9)	S(2)–O(1)–Mn(1)	136.31(17)
F(5)–Mn(2)–O(4)	95.35(9)	S(1)–O(2)–Mn(1)#2	125.93(15)
F(6)–Mn(2)–O(4)	84.71(9)	Mn(2)–F(5)–Mn(3)#4	130.52(10)
O(3)–Mn(2)–O(4)	168.20(11)	Mn(3)–F(6)–Mn(2)	124.83(10)
F(4)#3–Mn(3)–F(6)	87.42(9)	S(1)–O(3)–Mn(2)	134.42(16)
F(4)#3–Mn(3)–F(2)#2	171.13(8)	S(2)–O(4)–Mn(2)	126.28(15)
F(6)–Mn(3)–F(2)#2	93.88(9)	S(2)–O(5)–Mn(3)#4	126.19(16)
F(4)#3–Mn(3)–F(5)#3	91.66(9)	S(1)–O(6)–Mn(3)	124.99(15)
C(2)#5–C(1)–N(3)	108.9(3)	C(4)#6–C(3)–N(4)	110.4(3)
C(2)–N(3)–C(1)	110.1(3)	C(4)–N(4)–C(3)	109.8(3)
C(1)#5–C(2)–N(3)	112.0(3)	N(4)–C(4)–C(3)#6	111.5(3)

^a Symmetry transformations used to generate equivalent atoms: #1 *x*, *−y* + 1/2, *z* − 1/2; #2 *x*, *−y* + 1/2, *z* + 1/2; #3 *x*, *y* − 1, *z*; #4 *x*, *y* + 1, *z*; #5 *−x*, *−y*, *−z* + 2; #6 *−x* + 1, *−y* − 1, *−z* + 2.

atoms, the value being in the range 0.64–0.66. Thus, the framework stoichiometry of $[\text{Mn}^{\text{II}}_3\text{F}_6(\text{SO}_4)_2]$ with a 4– charge requires the amine to be doubly protonated alongside the presence of two ammonium ions. The anionic Kagome sheets of $[\text{Mn}^{\text{II}}_3\text{F}_6(\text{SO}_4)_2]^{4-}$ are stacked one over the other in an ABAB fashion and are held strongly by the hydrogen bond interaction of the amine and ammonium ions residing in the inter-layer space (Fig. 2). The amine and the ammonium ions form $\text{N}-\text{H}\cdots\text{O}$ ($\theta_{[\text{N}-\text{H}\cdots\text{O}]} = 104\text{--}173(4)^\circ$, $d(\text{N}\cdots\text{O}) = 2.936(4)\text{--}2.940(5)$ Å), $\text{N}-\text{H}\cdots\text{F}$ ($\theta_{[\text{N}-\text{H}\cdots\text{F}]} = 126\text{--}177(3)^\circ$, $d(\text{N}\cdots\text{F}) = 2.770(4)\text{--}3.128(4)$ Å), $\text{C}-\text{H}\cdots\text{O}$ ($\theta_{[\text{C}-\text{H}\cdots\text{O}]} = 102\text{--}164^\circ$, $d(\text{C}\cdots\text{O}) = 2.770(4)\text{--}3.210(4)$ Å) and $\text{C}-\text{H}\cdots\text{F}$ hydrogen bonds ($\theta_{[\text{C}-\text{H}\cdots\text{F}]} = 138\text{--}152^\circ$, $d(\text{C}\cdots\text{F}) = 3.215(4)\text{--}3.402(4)$ Å) with the framework oxygens and fluorines.

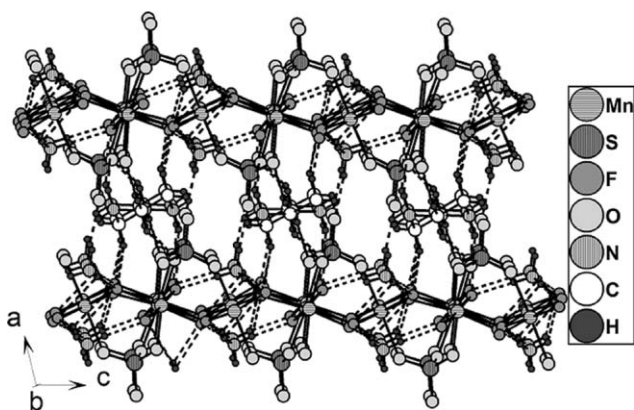


Fig. 2 Structure of $[\text{C}_4\text{N}_2\text{H}_{12}][\text{NH}_4]_2[\text{Mn}^{\text{II}}_3\text{F}_6(\text{SO}_4)_2]$, **I**, showing the stacking of layers and the presence of piperazine in the interlayer space.

Thermogravimetric analysis of **I** showed a two-step weight loss, the first loss corresponding to the loss of ammonia, amine and HF in the range 130–400 °C (obs. = 32.6%, calc. = 33.6%). The second weight loss occurs in the 460–850 °C range (obs. = 31%, calc. = 28%). The end product was found to be Mn_3O_4 (JCPDS file card PDF # 00-001-1127).

Magnetic properties

We show the variable temperature magnetic susceptibility (χ) data of **I** recorded at 100 and 1000 Oe in Fig. 3. In the paramagnetic region, the susceptibility follows the Curie–Weiss law with a negative Weiss temperature of 30 K as obtained from the fit of the χ_{M}^{-1} data in the 100–300 K range (inset of Fig. 3a). The negative θ_{p} value suggests that the exchange interaction is antiferromagnetic. This θ_{p} value is lower than that of the Fe^{3+} Kagome compounds (>600 K). The effective magnetic moment of Mn is $5.96\mu_{\text{B}}$, almost equal to the spin only $S = 5/2$ value of $5.92\mu_{\text{B}}$ since there is negligible orbital contribution to the moment and it is comparable to that of manganese(II) compounds reported in the literature.⁸ The field-cooled (FC) and the zero-field cooled (ZFC) magnetic susceptibility data measured at 100 Oe show little difference as can be seen from Fig. 3(b). The susceptibility data reveal a shoulder around 10 K which becomes broader as the magnetic field is increased to 1000 Oe. The susceptibility data do not change significantly with the field and the compound does not show any magnetic polarization at higher magnetic fields. This behavior suggests that the material is essentially paramagnetic with antiferromagnetic (AFM) interaction exhibiting only short-range order. Long-range AFM

order would have given a sharp transition as in the Fe^{3+} jarosites. The linear field dependence of magnetization at low temperatures (see inset of Fig. 3b) also supports the above observations.

Conclusions

An amine-templated Mn^{2+} sulfate with the Kagome structure, which is the first example of a $S = 5/2$ Kagome compound analogous to the well-known Fe^{3+} jarosites has been synthesized under solvothermal conditions. In the Mn^{2+} Kagome compound, **I**, studied by us, we do not observe any magnetic frustration or long-range AFM ordering as in the other $S = 5/2$ and other integer spins Kagome compounds. The absence of any ferromagnetic interaction in **I** is in accordance with theoretical predictions, which require integer spins to metal ions. It is noteworthy that the Co^{2+} ($S = 3/2$) and Cr^{3+} ($S = 3/2$) compounds with the Kagome structure have properties comparable to those of the analogous Fe^{3+} jarosites.^{9,10} A pure $S = 1/2$ copper Kagome compound is reported to exhibit spin frustration.¹¹

Experimental

Synthesis and characterization

In a typical synthesis of $[\text{C}_4\text{N}_2\text{H}_{12}][\text{NH}_4]_2[\text{Mn}^{\text{II}}_3\text{F}_6(\text{SO}_4)_2]$, **I**, 0.502 g of $\text{Mn}(\text{NO}_3)_2 \cdot 4\text{H}_2\text{O}$ was dissolved in 4.6 ml of ethylene glycol (EG) under constant stirring. To this mixture, 0.22 ml of sulfuric acid (H_2SO_4 , 98%) and 0.344 g of piperazine (PIP) were added, followed by the addition of 0.35 ml HF (40%). The resultant mixture with a molar composition of $2\text{Mn}(\text{NO}_3)_2 \cdot 4\text{H}_2\text{O} : 4\text{H}_2\text{SO}_4 : 4\text{PIP} : 80\text{EG} : 8\text{HF}$ had an initial pH < 2 after stirring for 2 h. The mixture was taken in a 23 ml PTFE-lined acid digestion bomb and heated at 150 °C for 3 d. After cooling to room temperature, the product containing colorless hexagonal crystals (yield: 50% with respect to Mn) was filtered off and washed with water and then with ethanol.

I was characterized by powder X-ray diffraction (PXRD), energy dispersive analysis of X-rays (EDAX), chemical analysis, thermogravimetric analysis (TGA) and IR spectroscopy. EDAX analysis indicated the ratio of Mn : S to be 3 : 2. The presence of fluorine was confirmed by analysis and the percentage of fluorine estimated by EDAX in a field emission scanning electron microscope was also satisfactory. Thermogravimetric analysis also confirms the stoichiometry of the compound. Bond valence sum calculations⁶ and the absence of electron density near fluorine in the difference Fourier map also provide evidence for the presence of fluorine. The sulfate content was found to be 30.8% compared to the expected 32% on the basis of the formula.

The IR spectrum of **I** showed characteristic bands for the amine as well as the ammonium moieties. The ammonium ions result from the decomposition of the piperazine molecules used in the starting synthesis mixture. The stretching mode of the $-\text{N}-\text{H}$ bond (of the amine) is observed around 3004 cm^{-1} (ν_1). The $\text{N}-\text{H}$ bending modes of the amine and NH_4^+ are observed in the range $1440\text{--}1586\text{ cm}^{-1}$. Strong bands in the region $850\text{--}1015\text{ cm}^{-1}$ correspond to ν_1 and ν_3 while bands in the region $583\text{--}644\text{ cm}^{-1}$ can be assigned to ν_2 and ν_4 fundamental modes of the sulfate ion.¹²

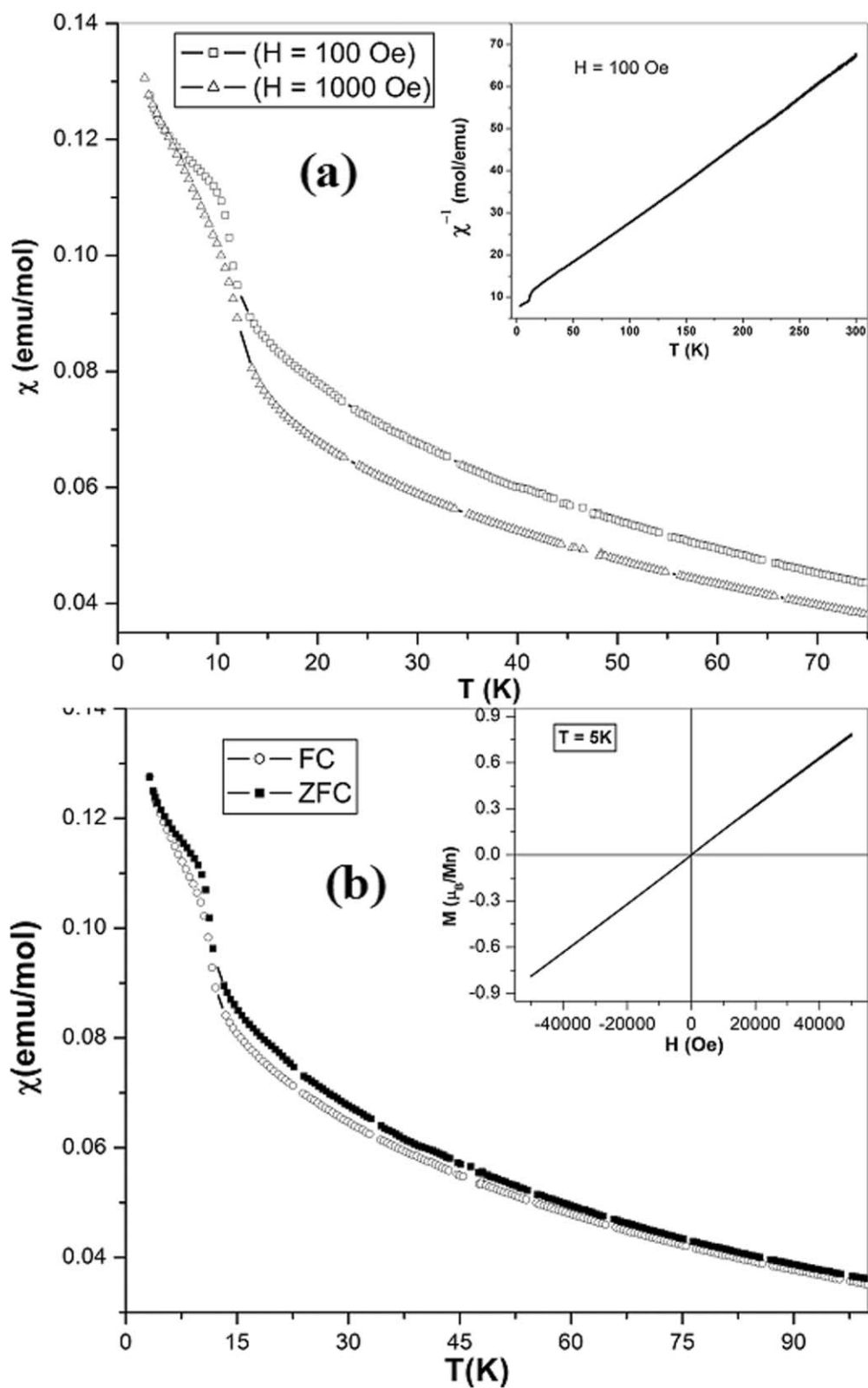


Fig. 3 (a) Temperature variation of χ of $[\text{C}_4\text{N}_2\text{H}_{12}][\text{NH}_4]_2[\text{Mn}^{13}\text{F}_6(\text{SO}_4)_2]$, **I** under ZFC conditions ($H = 100$ and 1000 Oe). Inset shows the variation of inverse susceptibility. (b) Temperature dependence of the magnetic susceptibility of **I** under field-cooled (FC) and zero-field-cooled (ZFC) conditions (100 Oe). Inset shows the M - H curve at 5 K.

Table 2 Crystal data and structure refinement parameters for **I**

Empirical formula	C ₄ H ₂₀ F ₆ Mn ₃ N ₄ O ₈ S ₂
Crystal system	Monoclinic
Space group	<i>P</i> 2(1)/ <i>c</i>
Crystal size/mm	0.2 × 0.16 × 0.08
<i>a</i> /Å	17.6128(2)
<i>b</i> /Å	7.60040(10)
<i>c</i> /Å	13.05010(10)
β /°	104.8680(10)
<i>V</i> /Å ³	1688.45(3)
<i>Z</i>	4
Formula mass	595.20
ρ_{calc} /g cm ⁻³	2.342
λ (MoK α)/Å	0.71073
μ /mm ⁻¹	2.566
θ range/°	1.20 to 25.68
Total data collected	18444
Limiting indices	-21 ≤ <i>h</i> ≤ 21, -9 ≤ <i>k</i> ≤ 7, -15 ≤ <i>l</i> ≤ 15
Unique data	3197
Refinement method	Full-matrix least squares on <i>F</i> ²
<i>R</i> _{int}	0.0377
<i>R</i> [<i>I</i> > 2 σ (<i>I</i>)]	<i>R</i> ₁ ^a = 0.0324, <i>wR</i> ₂ ^b = 0.0862
<i>R</i> (all data)	<i>R</i> ₁ = 0.0417, <i>wR</i> ₂ = 0.0924
Goodness of fit (<i>S</i>)	1.044
Largest difference map peak and hole/e Å	0.739 and -0.786

^a $R_1 = \sum |F_o| - |F_c| / \sum |F_o|$; ^b $wR_2 = \{[w(F_o^2 - F_c^2)]/[w(F_o^2)]\}^{1/2}$, $w = 1/[\sigma^2(F_o^2) + (aP)^2 + bP]$; $P = F_o^2 + 2F_c^2/3$; where $a = 0.0367$ and $b = 6.0435$.

Magnetic measurements were performed at temperatures between 2 and 300 K, in a vibrating sample magnetometer using a physical property measurement system (quantum design).

Single-crystal structure determination

Single crystal structure determination by X-ray diffraction was performed at 298 K on a Bruker AXS-CCD diffractometer equipped with a normal focus, 2.4 kW sealed-tube X-ray source (Mo-K α radiation, $\lambda = 0.71073$ Å) operating at 40 kV and 40 mA. The structure was solved by direct methods using SHELXS-97.¹³ An empirical absorption correction based on symmetry equivalent reflections was applied using SADABS.¹⁴ All the hydrogen positions of the ammonium ions were found in the difference Fourier maps. For the final refinement, hydrogen atoms of the amine were placed geometrically and held in the riding mode. Full-matrix least-squares structure refinement against |*F*²| was carried out using the SHELXL-97 package of programs.¹⁵ Details of the structure determination and final refinements for **I** are listed in Table 2. The positions of the fluorine atoms in **I** were

located primarily by looking at their thermal parameters. Assigning them as oxygen instead of fluorine invariably leads to non-positive definite values when they were refined with anisotropic displacement parameters. The powder X-ray diffraction pattern of **I** was in good agreement with the simulated pattern based on the single-crystal data, indicative of phase purity.

CCDC reference number 621801.

For crystallographic data in CIF or other electronic format see DOI: 10.1039/b613732f

Acknowledgements

JNB thanks CSIR, India for a senior research fellowship.

References

- (a) A. P. Ramirez, *Annu. Rev. Mater. Sci.*, 1994, **24**, 453; (b) J. E. Greedan, *J. Mater. Chem.*, 2001, **11**, 37; (c) D. G. Nocera, B. M. Bartlett, D. Grohol, D. Papoutsakis and M. P. Shores, *Chem.–Eur. J.*, 2004, **10**, 3850; (d) A. S. Wills, A. Harrison, C. Ritter and R. I. Smith, *Phys. Rev. B: Condens. Matter*, 2000, **61**, 6156; (e) A. S. Wills and A. Harrison, *J. Chem. Soc., Faraday Trans.*, 1996, **92**, 2161.
- (a) B. M. Bartlett and D. G. Nocera, *J. Am. Chem. Soc.*, 2005, **127**, 8985; (b) D. Grohol, D. G. Nocera and D. Papoutsakis, *Phys. Rev. B: Condens. Matter*, 2003, **67**, 064401.
- (a) D. Papoutsakis, D. Grohol and D. G. Nocera, *J. Am. Chem. Soc.*, 2002, **124**, 2647; (b) D. Grohol, D. Papoutsakis and D. G. Nocera, *Angew. Chem., Int. Ed.*, 2001, **40**, 1519.
- J. N. Behera and C. N. R. Rao, *J. Am. Chem. Soc.*, 2006, **128**, 9334.
- S. K. Pati and C. N. R. Rao, *J. Chem. Phys.*, 2005, **123**, 234703.
- B. Gerand, G. Nowogrocki, J. Guenot and M. Figlarz, *J. Solid State Chem.*, 1979, **29**, 429.
- I. D. Brown and D. Altermatt, *Acta Crystallogr., Sect. B*, 1985, **41**, 244.
- (a) Z. A. D. Lethbridge, M. J. Smith, S. K. Tiwary, A. Harrison and P. Lightfoot, *Inorg. Chem.*, 2004, **43**, 11; (b) Z. A. D. Lethbridge, A. F. Congreve, E. Esslemont, A. M. Z. Slawin and P. Lightfoot, *J. Solid State Chem.*, 2003, **172**, 212.
- J. N. Behera, G. Paul, A. Choudhury and C. N. R. Rao, *Chem. Commun.*, 2004, 456.
- (a) S.-H. Lee, C. Broholm, M. F. Collins, L. Heller, A. P. Ramirez, Ch. Kloc, E. Bucher, R. W. Erwin and N. Lacey, *Phys. Rev. B: Condens. Matter*, 1997, **56**, 8091; (b) A. Keren, K. Kojima, L. P. Le, G. M. Luke, W. D. Wu, Y. J. Uemura, M. Takano, H. Dabkowska and M. J. P. Gingras, *Phys. Rev. B: Condens. Matter*, 1996, **53**, 6451.
- M. P. Shores, E. A. Nytko, B. M. Bartlett and D. G. Nocera, *J. Am. Chem. Soc.*, 2005, **127**, 13462.
- K. Nakamoto, *Infrared and Raman Spectra of Inorganic and Coordination Compounds*, Wiley, New York, 1978.
- G. M. Sheldrick, *SADABS Siemens Area Detector Absorption Correction Program*, University of Göttingen, Göttingen, Germany, 1994.
- (a) G. M. Sheldrick, *SHELXS-97 Program for crystal structure determination*, University of Göttingen, Göttingen, Germany, 1997; (b) G. M. Sheldrick, *Acta Crystallogr.*, 1990, **35**, 467.
- G. M. Sheldrick, *SHELXTL-97 Program for Crystal Structure Solution and Refinement*, University of Göttingen, Göttingen, Germany, 1997.